

Parallel Platform for Multi-Scale CFD Storm Flood Forecast Using Geographical Information System Applications

Tian Wan ^{a*} and Shahrouz Aliabadi ^{a†‡}

*a Northrop Grumman Center for HPC of Ship Systems Engineering,
Jackson State University, MS e-Center,
Box 1400, 1230 Raymond Road, Jackson, MS 39204, U.S.A.*

Keywords: parallel, multi-scale, ocean simulation, flood modeling

1. INTRODUCTION

This paper addresses one aspect of an on-going project at Jackson State University regarding homeland security in the state of Mississippi. The project proposes an integrated tool for multi-scale storm surge and flood forecast, as well as evaluation of the flood damage on coastal infrastructure including transportation systems in the three counties in Mississippi state. Specifically, this paper describes the storm surge and wave models used for hurricane forecast and simulation, and the methodology that we use to integrate the results from flood modeling into geographical information systems for visualization, analysis and decision-making.

The simulation and prediction of storm surges and waves are intrinsically complex due to the interaction of a wide range of fluid motions, ranging from large-scale tide and wave to small-scale street level turbulence. Multi-scale flood simulation becomes a reality due to the rapid development of computer technology, the maturity of computational simulation models, and the public available database such as hurricane forecast advisories and geographical data. A suite of state-of-the-art models are integrated and the results will be presented in the paper. Namely, sea surface elevation, wind forcing and coastal currents are modeled using the fully nonlinear, two-dimensional, barotropic hydrodynamic model ADCIRC-2DDI (ADvanced CIRCulation Model, two Dimensional Depth-Integrated) [1]; the open-source, third-generation spectral wave prediction model SWAN (Simulation of WAVes in Near-shore area. [2]) is run interactively with ADCIRC. Both ADCIRC and SWAN run on an eight-core Mac Pro workstation using MPI and will be ported to other clusters as well. The predicted wave profile will be imported into our CFD solver CaMEL hybrid [3] that uses a hybrid finite volume and finite element method for solving incompressible free-surface flows. The CFD prediction results will be then imported into GIS software and Google Earth using computer graphics techniques.

In the following sections of the abstract, the storm surge and wave models are reviewed briefly, followed by the scalability test of the two models on an eight-core Mac Pro workstation.

* Postdoctoral Research Associate

† Professor and Director

‡ Correspondence to: Shahrouz Aliabadi, Northrop Grumman Center for HPC of Ship Systems Engineering, Jackson State University, MS e-Center Box 1400, 1230 Raymond Road, Jackson, MS 39204. U.S.A.

A node re-arrangement technique is also used to speed up the computation. Then the models are applied to forecast and simulation of hurricanes and tropical storms in the Gulf of Mexico. The parameters and oceanography data that we used for model setup are also described in this section. Hurricane Katrina is chosen as a test case, and our computed surge and wave results are compared with observed data. In the final paper, a database of past hurricanes and tropical storms near the coast of Mississippi will be demonstrated. Also published hurricane forecast advisories from National Hurricane Center will be parsed for practice forecast simulations. In the last section of the abstract, the method of converting different data formats and data visualization in Geographical Information System (GIS) packages and Google Earth is discussed.

2. NUMERICAL MODELS

Sea surface elevation, wind forcing and coastal currents are modeled using the fully nonlinear, two-dimensional, barotropic hydrodynamic model ADCIRC-2DDI. ADCIRC-2DDI uses the depth-integrated equations of mass and momentum subject to the incompressibility, Boussinesq, and hydrostatic pressure approximations. Baroclinic processes were neglected, including any expansion and contraction due to radiational heating. The governing continuity and momentum equations are written in primitive form as:

$$\frac{\partial \xi}{\partial t} + \frac{1}{R \cos \phi} \left[\frac{\partial UH}{\partial \lambda} + \frac{\partial (VH \cos \phi)}{\partial \phi} \right] = 0 \quad (1)$$

$$\frac{\partial U}{\partial t} + \frac{1}{R \cos \phi} U \frac{\partial U}{\partial \lambda} + \frac{V}{R} \frac{\partial U}{\partial \phi} - \left(\frac{\tan \phi}{R} U + f \right) V = -\frac{1}{R \cos \phi} \frac{\partial}{\partial \lambda} \left[\frac{p_s}{\rho_0} + g(\xi - \alpha \eta) \right] + \frac{\tau_{s\lambda}}{\rho_0 H} - \tau_* U \quad (2)$$

$$\frac{\partial V}{\partial t} + \frac{1}{R \cos \phi} U \frac{\partial V}{\partial \lambda} + \frac{V}{R} \frac{\partial V}{\partial \phi} + \left(\frac{\tan \phi}{R} U + f \right) U = -\frac{1}{R} \frac{\partial}{\partial \phi} \left[\frac{p_s}{\rho_0} + g(\xi - \alpha \eta) \right] + \frac{\tau_{s\phi}}{\rho_0 H} - \tau_* V \quad (3)$$

Equation (1) is the continuity equation, and (2) and (3) are the momentum equations in λ (degrees longitude) and ϕ (degrees latitude) direction. The variables are defined as: ξ = free-surface elevation relative to the geoid; U , V = depth-averaged horizontal velocities; $H = \xi + h$ = total water column; h = bathymetric depth relative to the geoid; $f = 2\Omega \sin \phi$ = Coriolis parameter; Ω = angular speed of the Earth; p_s = atmospheric pressure at the free surface; g = acceleration due to gravity; η = Newtonian equilibrium tide potential; α = effective Earth elasticity factor; ρ_0 = reference density of water; $\tau_{s\lambda}$, $\tau_{s\phi}$ = applied free-surface stress; $\tau_* = C_f (U^2 + V^2)^{1/2} / H$, and C_f = bottom friction coefficient. In this paper, a hybrid form of the standard quadratic parameterization for bottom stress is used that provides a friction factor that increases as the depth decreases in shallow water, similar to a Manning relationship. The parameters that are used for the Newtonian equilibrium tide potential are taken from the Eastcoast data set [4]. The applied free-surface stress is computed by SWAN and imported to ADCIRC every 30 minutes.

The third-generation wave model SWAN is chosen for use in this paper. SWAN solves the spectral action balance equation without any *a priori* restrictions on the spectrum for the evolution of wave growth. The equation represents the effects of spatial propagation, refraction, shoaling, generation, dissipation and nonlinear wave-wave interaction. The basic scientific philosophy of SWAN is identical to that of WAM cycle 3 [5]. While WAM uses explicit

propagation schemes in geographical and spectral spaces, SWAN employs implicit schemes that enable it to use very small grid size. Hence, SWAN is suitable for our applications in coastal regions. The SWAN Cycle III version 40.51 is used in the present paper, which solves the action balance equation:

$$\frac{\partial N}{\partial t} + \nabla_{\vec{x}} \cdot [(\vec{c}_g + \vec{U})N] + \frac{\partial \alpha_\sigma N}{\partial \sigma} + \frac{\partial \alpha_\theta N}{\partial \theta} = \frac{S_{\text{tot}}}{\sigma} \quad (4)$$

Here, $N(\vec{x}, t; \sigma, \theta)$ is the action density, defined as the ratio of wave energy density to the frequency, in space \vec{x} and time t , distributed over frequencies σ (as observed in a frame of reference moving with current velocity) and propagation direction θ (the directional normal to the wave crest of each spectral component). $\vec{c}_g = \partial \sigma / \partial \vec{k}$ is the wave number vector, and \vec{U} is the ambient current velocity. c_σ and c_θ are the propagation velocities in spectral space (σ , θ). S_{tot} in the right-hand side is the source term that represents all physical processes that generate, dissipate, or redistribute wave energy. In the present paper, we use the spherical coordinates format of the Equation (4):

$$\frac{\partial N}{\partial t} + \frac{\partial \alpha_\lambda N}{\partial \lambda} + \cos^{-1} \phi \frac{\partial \alpha_\phi \cos \phi N}{\partial \phi} + \frac{\partial \alpha_\sigma N}{\partial \sigma} + \frac{\partial \alpha_\theta N}{\partial \theta} = \frac{S_{\text{tot}}}{\sigma} \quad (5)$$

with longitude λ and latitude ϕ . The current velocity, water elevation and wind forcing are computed by ADCIRC and imported to SWAN every 30 minutes.

3. SIMULATION OF HURRICANE KATRINA

While a database of simulations of past hurricanes in the Gulf of Mexico will be established during the project, hurricane Katrina is chosen as a test case to be presented in the paper, considering the scope of its impact. Katrina strengthened from a low-end Category 3 hurricane to a Category 5 in less than 12 h, reaching an intensity of 145 kt by 1200 UTC 28 August, and attained its peak intensity of 150 kt at 1800 UTC 28 August about 170 n mi southeast of the mouth of the Mississippi River [6]. It is crucial to have automated simulation tool with fast turn-around during real-time events. In the current project, the process from parsing hurricane forecast advisories to the final GIS software integration will be automated by scripting languages.

3.1. Model Setup

Two sets of grids with different resolutions are used for ADCIRC simulation. The coarse grid is taken from the WNAT tidal database, *Eastcoast 1995* [4] which consists of 31,435 nodes and 58,369 elements; based on the coarse grid, the dense grid has points locally clustered in the Gulf of Mexico and has a total size of 94,611 nodes and 181,583 elements. The bathymetry data for the coarse grid, which is built in the grid file, is a combination of ETOPO5 [7] bathymetry database and NOS sounding bathymetric database [8]. The bathymetric data for the dense grid is interpolated using the open-source tool GREDIT [9]. The tidal setup is taken from the tidal database FES95.2 [4] and the K_1 , O_1 , Q_1 , M_2 , S_2 , N_2 and K_2 constituents are taken into account. The time step is 30 seconds for the coarse grid and 3 seconds for the dense grid. The complete set of nonlinear shallow water equation with wetting/drying is used. The weighting factor in generalized wave continuity equation and the time weighting factor use the default values. The

horizontal eddy viscosity chosen is $5 \text{ m}^2/\text{s}$. The parameters for treatment of the wetting/drying boundary are chosen to be 0.02 m for the minimum water depth, 10 for the minimum number of dry time steps, 10 for the number of rewetting time steps, and 0.05 m/s for the minimum velocity for wetting. The hybrid bottom friction formulation is used to represent the increase of the drag coefficient as the water depth decreases in shallow water, and the default values are used for the drag coefficients. The hurricane track data is taken from National Hurricane Center, and the wind field data is generated by a PBL wind model. The wave radiation stress is taken from SWAN output. Tidal and default boundary conditions are used on open and land boundaries. Computation time is from 08/23/18Z to 08/30/03Z, 2005.

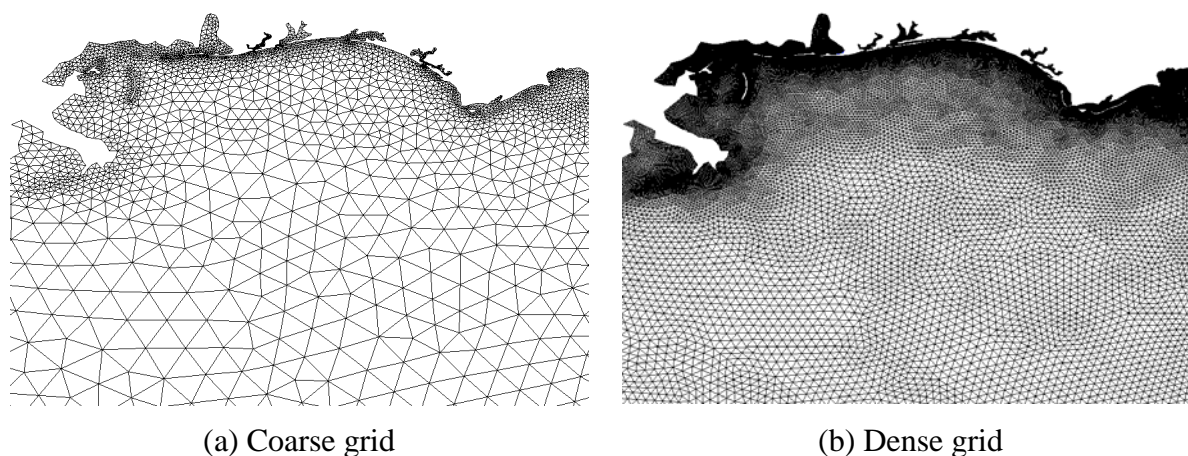


Figure 1. ADCIRC computational grid for the hurricane Katrina test case. Only the coastal region is shown.

The SWAN computation domain covers from 92 W to 80 W and from 24 N to 33 N, with 361 by 271 nodes. The 2-minute US Coastal Relief Model is used as bathymetry data. Wave generation, quadruplet and triad interactions, depth-limited wave breaking, and wave white capping are switched on. We choose 0.042 Hz as the lowest frequency and 1 Hz as the highest frequency, with a total of 41 frequencies and 36 directions. Both stationary and nonstationary computations are performed, from 08/27/00Z to 08/30/03Z, 2005. For stationary cases, computations are at every 30 minutes interval; for nonstationary computations time step of 5 minutes is used. The water elevation, current velocities and wind field are taken from ADCIRC every 30 minutes.

3.2. Computation Speed Test

In the final form of this paper, the scalability test of ADCIRC and SWAN will be presented, as well as a node reordering technique for Mac Pro. The preliminary scalability test results are plotted in Fig. 2.

3.3. Preliminary Results

The water elevation contours are plotted in Fig. 3 after hurricane Katrina made landfall. For visualization purpose, the NOAA NGDC GLOBE 1 km DEM data is plotted as well. It shows

that the maximum storm tide exceeds 7 m. Observed data from NOAA tide and current stations are compared with our ADCIRC computed results. The information of the stations is listed in Table 1. The computed water elevation with observed data at the four stations is plotted in Fig. 4. The plots show that our computation is able to predict the maximum storm tide. The maximum difference between our computed elevation and observed data occurs in one tidal period before the maximum storm tide. The reason for the difference will be examined in the final paper, by performing computation on much higher resolution grid on the local region. Note that the results on the dense grid don't improve the accuracy from those on the coarse grid, except that the coarse grid computation over-predicted the maximum storm tide at the Dauphin Island, AL and Grand Isle, LA stations. The reason why the results on both grids are the same on the other two stations is because both grids have the same resolution in those regions. In the final paper, localized computation will be conducted, which includes river inflow/outflow boundary conditions, and the results will be compared with the present ones.

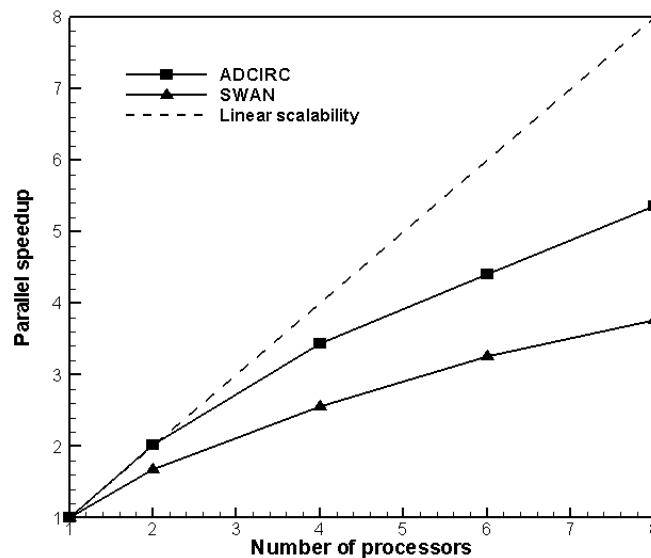


Figure 2. Scalability test results for the ADCIRC and SWAN model. The tests were conducted on a 94,611 nodes grid for ADCIRC and a 97,831 nodes grid for SWAN.

Station id	Name	Longitude	Latitude
8735180	Dauphin Island AL	-88.075	30.250
8761724	Grand Isle, LA	-89.957	29.263
8729840	Pensacola, FL	-87.212	30.403
8729108	Panama City, FL	-85.667	30.152

Table 1

NOAA tide and current stations referenced in the present paper.

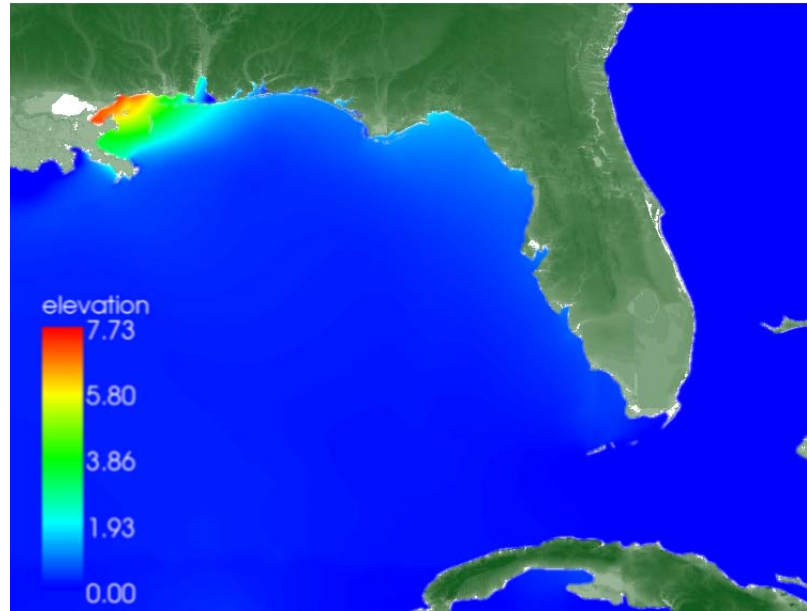
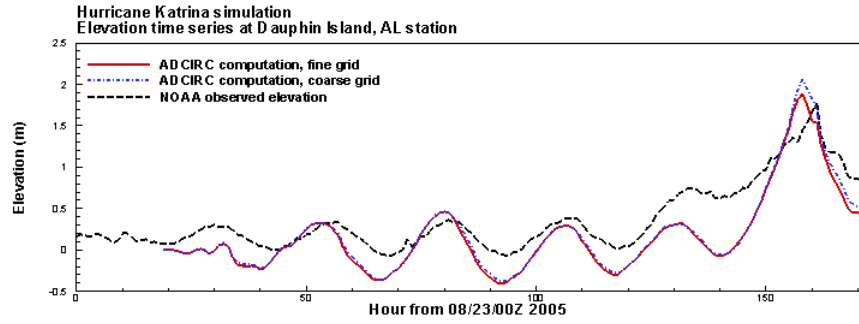


Figure 3. Computed water elevation contours by ADCIRC. The contours in the land points are plotted using NOAA NGDC GLOBE 1 km DEM data.

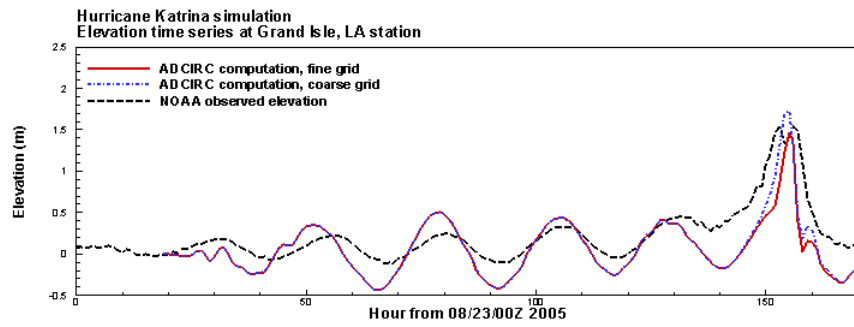
Both stationary and nonstationary computations are conducted using SWAN wave model. The stationary computation is performed at every 30 minutes till steady state, while the nonstationary computation solves for the unsteady wave field using time step of 5 minutes. The stationary computation is more efficient than nonstationary one and easier to integrate with ADCIRC model, however, its accuracy is of question when the SWAN computation domain is large. In the case of nonstationary computation, the way that ADCIRC interacts with SWAN is the following: firstly, ADCIRC computes for the whole simulation time, the computed water elevation, current velocities and wind field are imported into SWAN; at the second step, SWAN computes for the whole simulation time, and the computed wave radiation stress is imported into ADCIRC. This process iterates till convergence. In practice, two iterations of the cycle process show enough convergence.

The computed SWAN wave data are plotted in Fig. 5 and 6, at NDBC buoy station 42039 and 42040 respectively. The plots show that our computed data agree very well with the observed significant wave height, average wave period and dominate wave period. They also show that only nonstationary computation can simulate the unsteadiness of the wave field during hurricane.

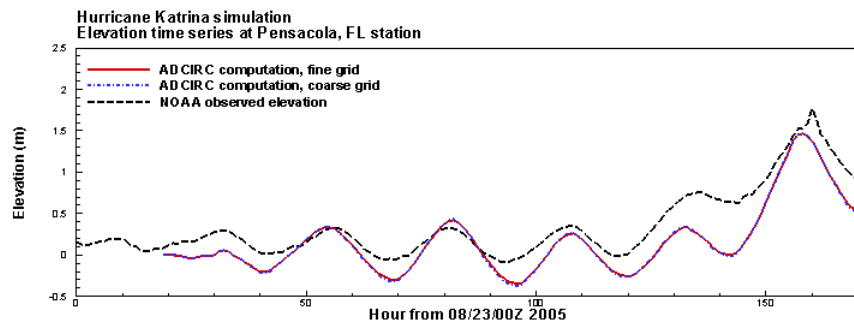
In the final paper, flood profiles will be imported to our CFD solver CaMEL hybrid. Flood impact force on selected building will be calculated as well.



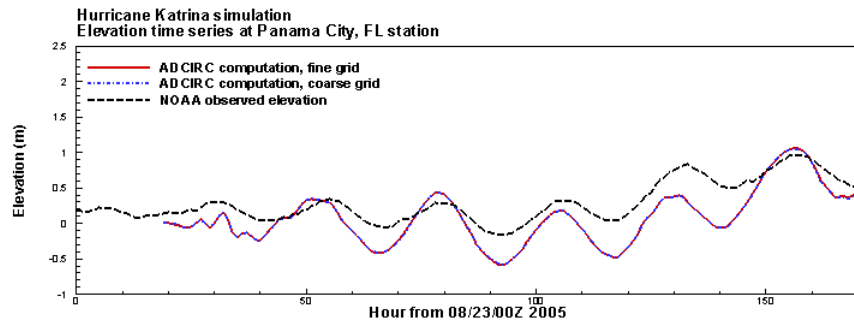
(a) Dauphin Island AL station



(b) Grand Isle LA station

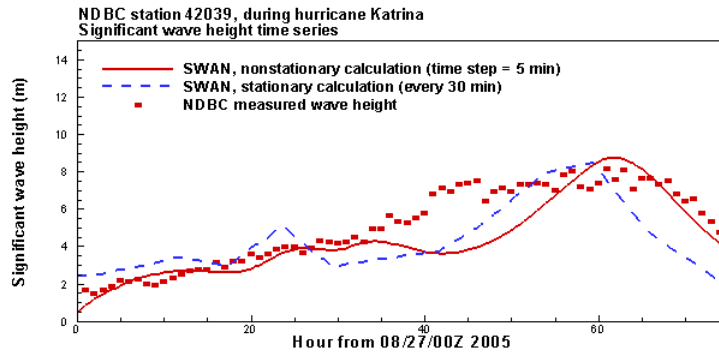


(c) Pensacola FL station

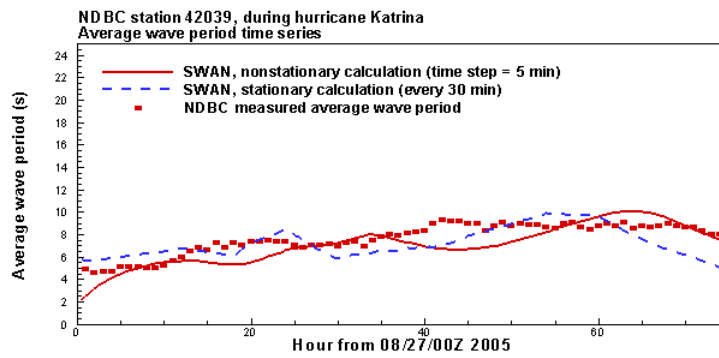


(d) Panama City FL station

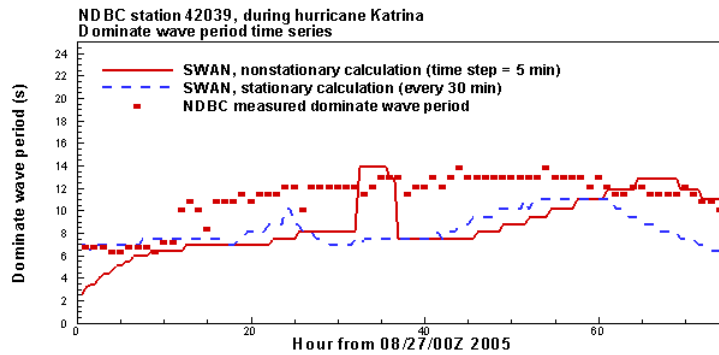
Figure 4. ADCIRC computed water elevation with NOAA observed data.



(a) Significant wave height

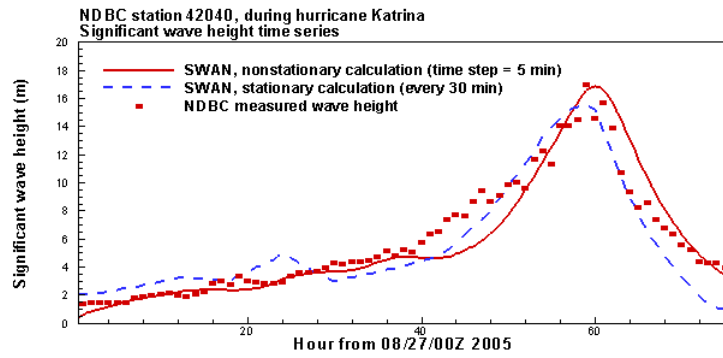


(b) Average wave period

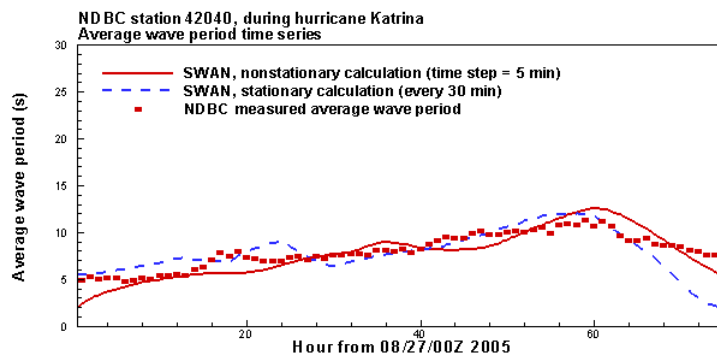


(c) Dominate wave period

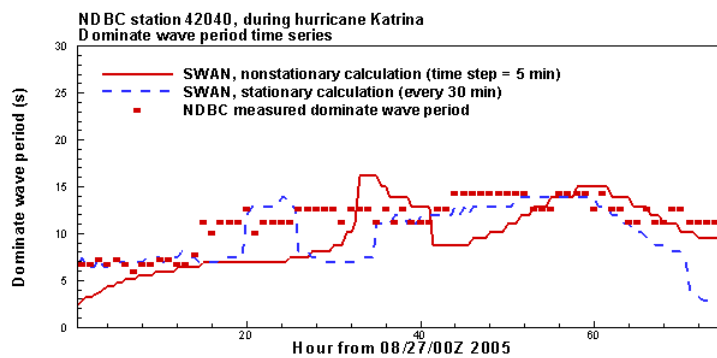
Figure 5. Computed wave data with observed data at NDBC buoy 42039.



(a) Significant wave height



(b) Average wave period



(c) Dominate wave period

Figure 6. Computed wave data with observed data at NDBC buoy 42040.

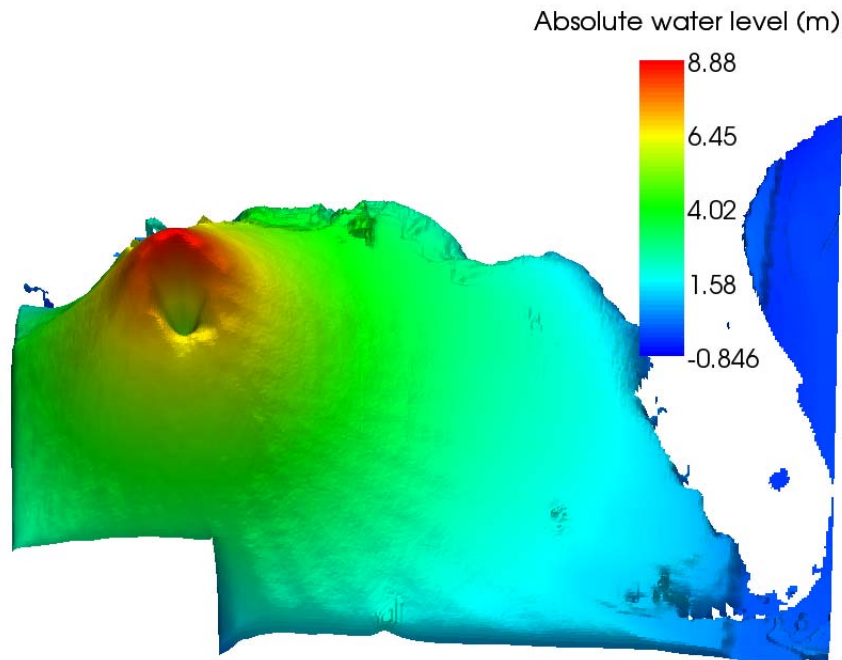


Figure 7. Isosurface of flood surface level stored in VRML format. The flood surface is computed as storm tide plus one half of the significant wave height.

4. GIS SOFTWARE INTEGRATION

There are basically two ways to import CFD results into GIS software, either in raster image format or in vector format. In the paper, CFD results are converted into a vector format, VRML 97 [10]. VRML can store the geometric information of the model in a similar way to the *de facto* industry standard STL. On the other hand, VRML stores less redundant data than STL, and can store two or more parts simultaneously in a single file. More importantly, VRML format data can be imported into our GIS software ArcGIS. An open-source Grass GIS software can also be in use. The data conversion is done by scripts written in Python. For example, to plot the flood level due to the combination of storm tide and wave, a script is written to extract data from computed results and perform quantitative analysis, followed by filtering out the land points and writing the data in VRML format. An example VRML formatted data is visualized in Figure 7.

In the final paper, both of the wave profile and CFD results will be imported to the GIS software and presented.

ACKNOWLEDGEMENT

Work is funded by the Department of Homeland Security. Partial support for this work is provided by Northrop Grumman Ship Systems.

REFERENCES

1. J. J. Westerink, R. A. Luetlich, C. A. Blain and N. W. Scheffner, ADCIRC: An advanced three-dimensional circulation model for shelves, coasts and estuaries. Report 2: Users' Manual for ADCIRC-2DDI. Technical Report DRP-94, U.S. Army Corps of Engineers.
2. N. Booji, R. C. Ris and L. H. Holthuijsen, A third-generation wave model for coastal regions. Part 1, Model description and validation. *Journal of Geophysical Research*, C4, 104, 7649-7666.
3. S. Tu and S. Aliabadi, Development of a hybrid finite volume/element solver for incompressible flows. *Int. J. Numer. Meth. Fluids* 2007; 55:177-203
4. A. Y. Mukai, J. J. Westerink, R. A. Luetlich, Jr., and D. Mark Eastcoast 2001, A tidal constituent database for western north Atlantic, Gulf of Mexico, and Caribbean Sea. U.S. Army Corps of Engineers, ERDC/CHL TR-02-24.
5. WAMDI Group (13 authors, including V. J. Cardone and J. A. Greenwood). The WAM model – a third generation ocean prediction model. *J. of Phys. Oceanog.* 18, 1775-1810.
6. R. D. Knabb, J. R. Rhome and D. P. Brown, Tropical cyclone report hurricane Katrina 23-30 August 2005, National Hurricane Center, 20 December 2005.
7. National Geophysical Data Center, National Oceanic and Atmospheric Administration, Boulder, CO, 80303-3328. World Wide Web page accessed on 2 May 2001, <http://edcwww.cr.usgs.gov/glis/hyper/guide/etopo5>.
8. National Ocean Service (NOS) 1997. www.ngdc.noaa.gov/mgg/fliers/97mgg02.html.
9. CORIE software, Center for Coastal and Land-Margin Research, Oregon Health and Science University.
10. www.vrml.org/Specifications/VRML97